Journal of MATERIALS RESEARCH

Article
DOI:10.1557/s43578-024-01389-3

Argatroban- and copper-modified polymers with improved thromboresistance and antimicrobial properties

Liana Azizova[1,2,a], Volodymyr Chernyshenko[3], Daria Korolova[3], Iain U. Allan[2,4], Sergey Mikhalovsky[5,6], Lyuba Mikhalovska[2]

[1] School of Dentistry, Cardiff University, Heath Park, Cardiff CF14 4XY, UK
[2] School of Pharmacy and Biomolecular Sciences, University of Brighton, Lewes Road, Brighton BN2 4GJ, UK
[3] Department of Protein Structure and Function, Palladin Institute of Biochemistry, NAS of Ukraine, Kyiv, Ukraine
[4] Dalgain Biomedical Ltd, 24 Sherwood Road, Seaford, East Sussex BN25 3EH, England, UK
[5] Chuiko Institute of Surface Chemistry, NAS of Ukraine, 17, General Naumov Str., Kyiv 03164, Ukraine
[6] ANAMAD Ltd., Sussex Innovation Centre, Science Park Square, Falmer, Brighton BN1 9SB, UK
[a] Address all correspondence to this author. e-mail: AzizovaL@cardiff.ac.uk

Received: 18 October 2023; accepted: 26 June 2024

This paper describes a novel approach the development of biocompatible polyvinyl chloride (PVC) and polyurethane (PU) polymers, modified with copper (II) ions followed by the immobilisation the thrombin inhibitor argatroban (AG) using dopamine chemistry. The surface loading of the immobilised AG was 6.06 µg cm^{-2} on PVC and 6.66 µg cm^{-2} on PU, confirmed by FTIR and inhibitor concentration measurements. Both AG/Cu-modified polymers produced NO by catalytically decomposing S-nitrosothiol, reaching NO levels in plasma of 0.59×10^{-10} mol cm^{-2} min^{-1} for AG/Cu-PVC and 0.51×10^{-10} mol cm^{-2} min^{-1} for AG/Cu-PU, matching endothelial cell-produced physiological levels. This modification improved the haemocompatibility of the polymers through thrombin inhibition and reduced platelet aggregation and adhesion. Additionally, both modified polymers inhibited *Staphylococcus aureus* adhesion, growth and viability, confirming their acquired antibacterial properties. Antibacterial activity against *Escherichia coli* was also observed. These results demonstrate that modifying PVC and PU surfaces with copper (II) and AG produced materials with dual antithrombotic and antibacterial functions.

Introduction

The use of polymeric medical devices is often associated with several complications, the foremost among these being infection and surface-induced thrombosis which cause the medical device failure. To improve polymer resistance to bacterial infection and to design more thromboresistant polymers, new methods of their surface modification have been persistently developed. The design of a nitric oxide (NO) releasing surface is considered to be among the most promising approaches. This concept is based on the knowledge that NO has various useful physiological functions in the human body such as antiplatelet, anti-inflammatory, vasodilation [1, 2] and inhibition of biofilm formation properties [3]. The key synthetic routes extensively studied during the last two decades are the incorporation of exogenous NO donors into the material coating [4] and a covalent attachment of NO donors to the surface of the coating [5–8]. The major constraints of these tactics is the short lifetime of NO release due to the limited surface loading capacity of NO donors, and their low stability in vivo [9]. More recent attempts to produce NO-generating biomaterials exploited the ability of some transition metals such as copper and selenium species to catalyse S-nitrosothiol (RSNO) decomposition resulting in NO production [10–13]. Since the endogenous RSNOs are always present in human blood at the physiological level, their catalytic decomposition could be used as the source of NO. This approach has been considered as the most promising for the local NO delivery at the blood/material interface.

In our previous work two Cu-modified polymers, polyvinyl chloride (PVC) and polyurethane (PU) able to generate NO, were produced. It was shown that copper (II) ions attached to the polymer surface could generate NO up to the physiological level [14].

However, significant challenges caused by a surface-induced thrombosis continue to be a complication for some blood-contacting devices such as catheters, heart valves, stents and pacemakers, which are a vital part of life saving treatment for thousands of patients daily. The primary event which triggers this complication is the fast adsorption of plasma proteins on the biomaterial surface after contacting with blood. The clotting factors, being adsorbed onto polymer surface, cause conversion of prothrombin into an active enzyme thrombin. Thrombin further converts the soluble blood protein fibrinogen into a solid fibrin network and the latter together with adhered platelets form a solid blood clot. To prevent thrombosis caused by blood-contacting devices, systematic antiplatelet/anticoagulant therapy has been applied in clinical practice alongside the use of medical devices. However, in some patient groups, the administration of anticoagulants can lead to uncontrolled bleeding which is a life-threatening complication by itself. Consequently, the surface modification that facilitates the local release of anticoagulants remains a promising strategy for preventing device-induced thrombosis.

The most common approach for obtaining an anticoagulant surface was, for many years, fabrication of the heparin-releasing surfaces [15]. However, it has drawbacks because an uncontrolled release of heparin can cause a heparin-induced thrombocytopenia (HIT) in some patient groups. Another adverse point is that heparin is an indirect thrombin inhibitor, and its inhibition activity depends on another plasma protein—antithrombin (AT).

A range of direct thrombin inhibitors, such as thrombomodulin, hirudin, bivalirudin and argatroban (AG) have been used as their ability to bind thrombin directly gives a more predictable anticoagulant response than heparin [16, 17]. To increase the biomaterial surface thromboresistance, some of these direct thrombin inhibitors including AG [3] were immobilised onto different polymers with varied success [18–26]. AG is a synthetic, FDA-approved drug with a reliable and predictable anticoagulant effect; so far it has been considered the best alternative for preventing fibrin clot formation on the blood-contacting device surface [17]. Argatroban has been reported as an effective anticlotting agent for the development of nonthrombogenic extracorporeal devices for patients with thrombocytopenia [3, 22]. Moreover, the surface-grafted AG can overcome issues associated with its hepatotoxicity during parenteral administration [27].

Another common cause of medical device failure is the bacterial infection. A number of NO-releasing polymeric materials were developed and studied for their antibacterial properties [28–30]. The nitric oxide-releasing surfaces demonstrated a significant antibacterial effect [31, 32]. NO exhibited a broad antibacterial effect against both gram-positive and gram-negative bacteria via multiple biochemical pathways [31, 33–35]. Although the exact mechanism of its antibacterial properties is not clear yet, some NO-releasing materials demonstrated more pronounced antibacterial effects than conventional antimicrobial agents; this approach also seems to avoid the issue of the bacterial resistance to other biocidal substances [36].

The aim of this research was to develop PVC and PU polymers with enhanced thromboresistance and antibacterial properties. It was achieved by attaching copper ions and the direct thrombin inhibitor argatroban to the polymer surfaces (Fig. 1). The validity of this approach was assessed by the ability of modified polymers to inhibit thrombin activity and reduce platelet adhesion and aggregation. An additional measure of their acquired functionality included the release of NO, a crucial

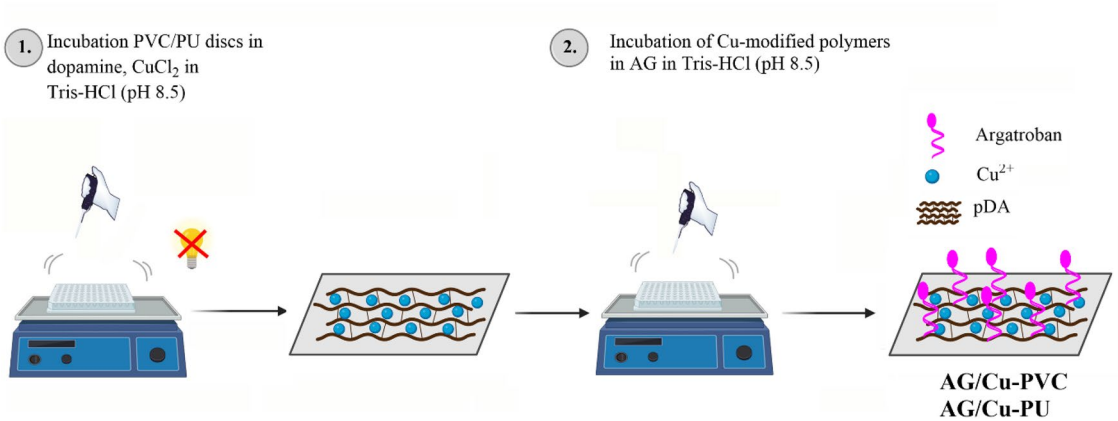

Figure 1: Visual depiction outlining the steps of modification.

factor for its vasodilatory and antiplatelet aggregation properties, which was tested under simulated physiological conditions.

The antibacterial performance of these modified polymers was also examined, with a focus on their ability to deter the adhesion and suppress the growth and viability of *Staphylococcus aureus* and *Escherichia coli*.

Results

Immobilisation of AG onto Cu-modified PVC and PU polymers

To prepare polymers with the dual antithrombotic and antibacterial function, two types of active substances were introduced to the polymer surface. One was the Cu(II) ions attached to the polymer surface for catalytic NO generation. The second substance was the direct thrombin inhibitor AG immobilised on the Cu-modified polymer surface. Two polymers, PVC and PU, were grafted with copper ions as described in our previous publication [14] using a dopamine coating technique. Dopamine polymerises into polydopamine (pDA) forming a stable thin film strongly attached to the polymer surface. It has high affinity with copper ions due to the large quantity of catechol groups. Next, AG was immobilised onto Cu-modified polymers. At this step, the quinone groups of the surface-adhered polydopamine film chemically bound AG by coupling with its primary amino group via Michael addition and Schiff base reactions. The concentration of AG before and after chemical coupling was measured by UV–Vis spectrophotometry at 333 nm (λ_{max}) and its remaining concentration in the solution was estimated using the molar extinction coefficient of 5000 M^{-1} cm^{-1} [37]. The amount of AG immobilised on the polymer surface was calculated from the difference in its concentration in the solution before and after incubation with polymer discs (Table 1).

TABLE 1: AG content on the surface of AG/Cu-modified PVC and AG/Cu-modified PU.

Sample	AG (nmol cm^{-2})	AG (μg cm^{-2})
AG/Cu-PVC	11.9 ± 1.3	6.05 ± 0.66
AG/Cu-PU	13.1 ± 0.3	6.66 ± 0.15

The attachment of Cu and AG to PVC and PU polymers was confirmed by assessing the chemical composition of the polymer surface using FTIR spectroscopy. The FTIR analysis of PVC and PU polymers was performed at each step of the modification (Fig. 2).

The IR spectra of PVC discs [Fig. 2(a)] contain a band at 2966 cm^{-1} typical of CH stretching vibrations and two bands at 2915 cm^{-1} and 2850 cm^{-1} related to CH_2 asymmetric stretching vibrations. The carbonyl band at 1737 cm^{-1} originates from

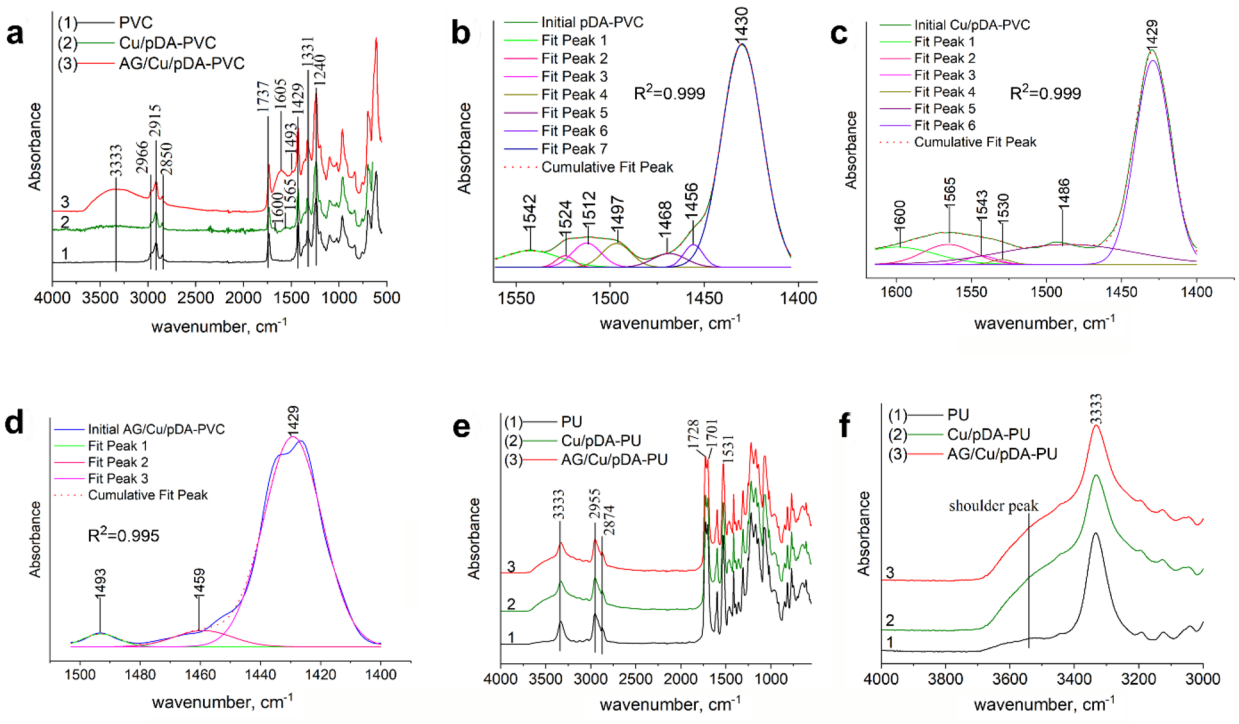

Figure 2: (a) Infrared spectra of PVC discs; (b) peak fitting of pDA-PU curves in the region 1600–1400 cm^{-1}; (c) peak fitting of Cu/pDA-PU curves in the region 1600–1400 cm^{-1}; (d) peak fitting of AG/Cu/pDA-PU curves in the region 1500–1400 cm^{-1}; (e) infrared spectra of PU discs; (f) infrared spectra of PU discs in the region 4000–3000 cm^{-1}.

the plasticiser employed [38]. The CH_2 deformation (bending) vibration band appeared in the spectrum at 1429 cm^{-1}. Bands at 1331 cm^{-1} and at 1240 cm^{-1} were assigned to CH_2 deformation and CH rocking vibration modes of PVC, respectively, while the C–Cl stretching vibrations are observed in the region of 600 cm^{-1}. These bands are characteristic bands of PVC.

FTIR analysis of pDA-PVC revealed characteristic bands within the 1600–1400 cm^{-1} range, displaying peaks at 1542 cm^{-1}, 1524 cm^{-1}, 1512 cm^{-1}, 1497 cm^{-1}, 1468 cm^{-1}, 1456 cm^{-1}, and 1430 cm^{-1} [Fig. 2(b)], corresponding to structural features of polydopamine. Modification with copper resulted in the Cu/pDA-PVC spectrum showing shifts and new bands at 1565 cm^{-1}, 1543 cm^{-1}, 1530 cm^{-1}, 1486 cm^{-1}, and 1429 cm^{-1} [Fig. 2(c)]. Further modification with AG (AG/Cu/pDA-PVC) introduced a distinct broad band at 3333 cm^{-1} [Fig. 2(a), spectrum 3]. In the case of PU, the IR spectrum of pristine PU [Fig. 2(e), spectrum 1] showed stretching vibration bands characteristic of the polymer's urethane structure. The modification of PU with Cu and AG [Fig. 2(e), spectra 2 and 3] was noted to maintain similar spectral profiles to non-modified PU, with a notable increase in intensity at 3333 cm^{-1}.

NO release

Data above showed that Cu ions are attached on both PVC and PU polymers. Although taking note that immobilisation of AG was carried out onto polymer surface with pre-immobilised cooper, this second step could obstruct access to the underlying copper ions, potentially reducing its capacity to generate NO. Valuation of NO generating activity by the final AG/Cu-modified material was necessary to confirm that Cu ions present on the polymer surface are able to generate NO from the NO source. Previously we showed the catalytic NO generation by Cu-modified PVC and PU polymers [14]. The evaluations carried out in PBS showed that AG/Cu-PVC and AG/Cu-PU polymers generated NO flux at the level of 1.66×10^{-10} mol cm^{-2} min^{-1} and 1.28×10^{-10} mol cm^{-2} min^{-1}, respectively [Fig. 3(a)]. As it seen from Fig. 3(a), the amount of NO generated by both modified polymers was significantly higher compared to their control polymers, respectively ($p < 0.0001$). In human blood plasma some reduction of NO flux for both AG/Cu-PVC and AG/Cu-PU polymers was observed [Fig. 3(b)], which could be explained by interference from various plasma proteins. Nevertheless, the measured NO amount produced by both AG/Cu-PVC and AG/Cu-PU polymers in plasma were statistically significantly higher than their respective controls in plasma ($p < 0.0001$), and importantly, these levels remained within the physiological range of NO produced by healthy endothelium, estimated between $0.5 - 4 \times 10^{-10}$ mol cm^{-2} min^{-1} [4]. These findings support the potential use of these modified polymers in biomedical applications where NO generation is desired.

Platelet adhesion and activation

The platelet adhesion and activation are important parameters for evaluation of biomaterials haemocompatibility. Upon contact with blood, adhesion of proteins to foreign material triggers platelet activation, which then bind to fibrin, forming clots. A significant number of adhered and spread platelets, as well as platelet–fibrin aggregates were present on the surface of

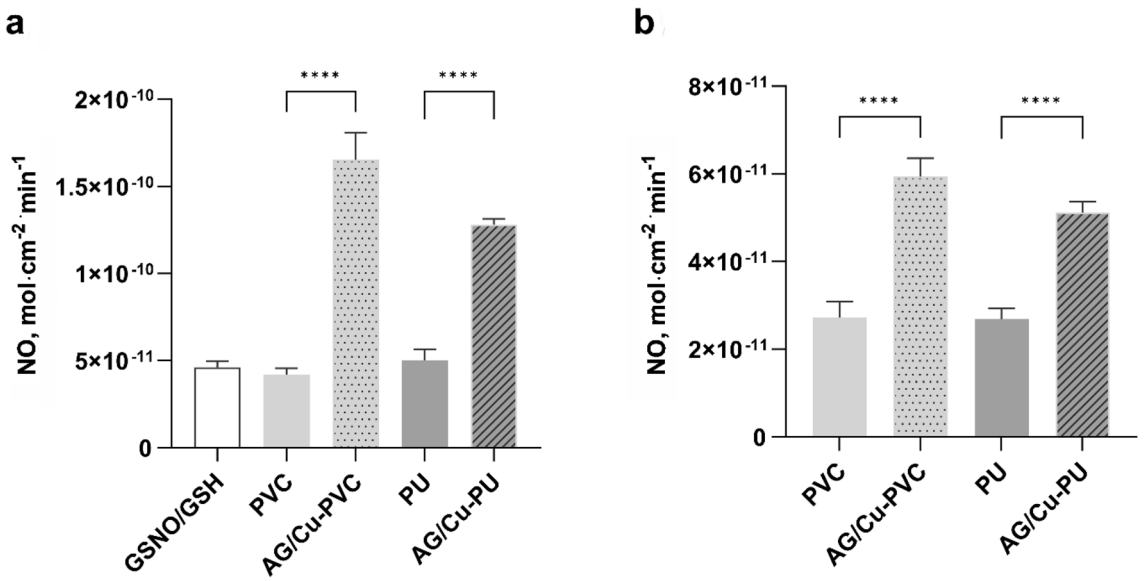

Figure 3: (a) NO generation after incubation of AG/Cu-modified polymers with 100 μM GSNO/GSH in PBS for 1 h. The values are mean of $n = 3$ measurements ± SD. (b) NO generation after incubation of AG/Cu-modified polymers with 100 μM GSNO/GSH in human plasma for 1 h. The values are mean of $n = 3$ measurements ± SD (****$p < 0.0001$ compared to controls).

non-modified PVC [Fig. 4(a)]. However, only a small number of platelets were observed on the AG-modified PVC surface [Fig. 4(b)]. Similarly, numerous activated and adhered platelets and platelet clumps were observed on the surface of non-modified PU [Fig. 4(c)], whereas few platelets, mostly round-shaped and without pseudopodia were found on the AG-modified PU polymer [Fig. 4(d)]. These data indicate that both AG/Cu-modified polymers reduced platelet adhesion and activation.

Inhibition of thrombin activity by AG/Cu-modified polymers

The thrombin inhibiting activity by AG/Cu-modified polymers was estimated after incubation of polymers with 0.32 NIH mL^{-1} of thrombin for 20 min in Tris–HCl buffer (TBS) or human blood plasma, followed by measuring of the residual thrombin activity. The last was calculated from the rate of the chromogenic thrombin substrate S2238 cleavage. Statistically significant decrease in thrombin activity was observed after incubation of either AG/Cu-modified PVC or AG/Cu-modified PU in buffered thrombin solution when compared to both unmodified polymers and to the thrombin control ($p < 0.0001$) [Fig. 5(a)].

The same method was applied to measure the ability of AG-modified polymers to inhibit thrombin in human platelet-poor blood plasma (PPP). In this case thrombin formation in plasma was initiated by the prothrombin activator from the *Echis carinatus multisquamatis* venom in situ [39, 40] and the residual thrombin activity was assessed with thrombin substrate S2238 after 20 min of incubation with polymer discs as above.

Both AG/Cu-modified polymers considerably decreased thrombin activity in plasma when compared with unmodified polymers [Fig. 5(b)].

When compared the thrombin inhibition by AG/Cu-modified polymers to the thrombin control in plasma, the PU modified samples showed higher inhibition than modified PVC. However, the less prominent difference between the modified PVC and a thrombin control could be explained by very high variation in the PVC samples measurement.

These results confirm that AG-modified polymers were able to inhibit thrombin activity in both, buffer solutions and human plasma. It could be also mentioned that the extent of this inhibition could varied depends on the initial polymer and the medium.

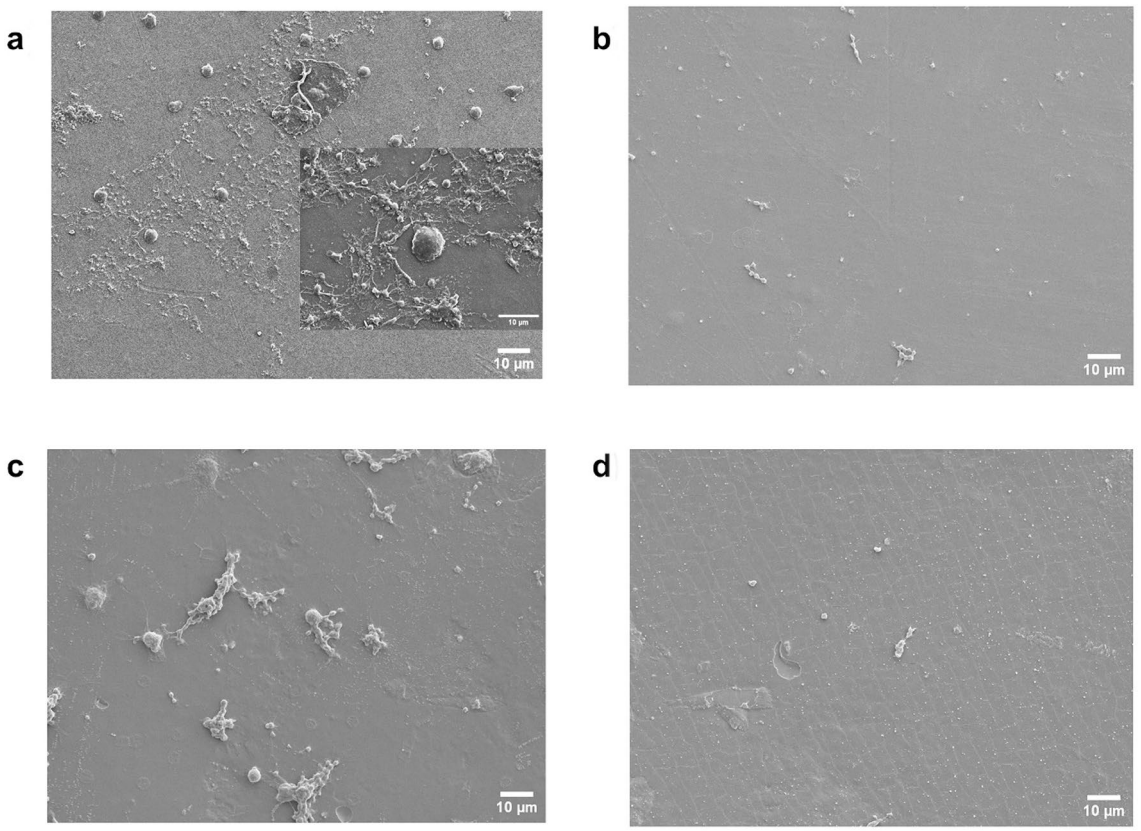

Figure 4: Representative SEM images of platelets adhered to the surface of polymers. (a) unmodified PVC, at ×2000 magnification (inset: PVC at 5000×); (b) AG/Cu-PVC, (c) unmodified PU and (d) AG/Cu-PU at ×2000 magnification. The polymer discs were incubated with human PRP for 2 h.

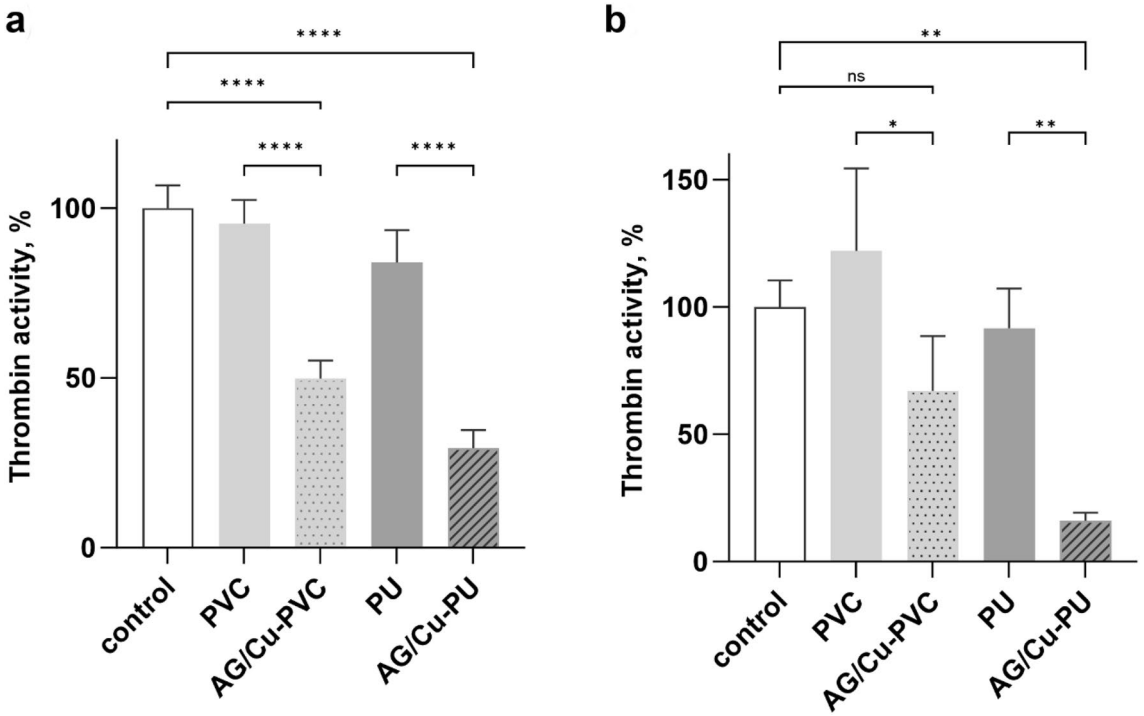

Figure 5: The residual thrombin activity after incubation with unmodified and Cu/AG-PVC and Cu/AG-PU modified polymer discs in (a) PBS and (b) platelet-poor human blood plasma. Substrate S2238 was added after incubation of polymer discs with 0.32 NIH/mL of thrombin for 20 min. The values are mean of $n = 3$ measurements ± SD (*$p < 0.05$, **$p < 0.01$, ***$p < 0.001$, ****$p < 0.0001$ compared to controls).

Platelet aggregometry

Platelet aggregation is one of the critical indicators of the blood clot formation and the platelet aggregometry method has been generally used for assessing the thrombogenicity of biomaterials. Both AG-modified polymers substantially decreased the thrombin-induced level and speed of platelet aggregation in the platelet-rich plasma (PRP) (Fig. 6). In the samples with AG-modified polymers, a small amount of platelet aggregation (up to 10%) was observed within the initial 50 s, followed by their disaggregation. Then, after about 150 s a very slow formation of insoluble fibrin occurred, whereas the visible fibrin clot was not fully formed during 500 s of measurement [Fig. 6(a, b)—red curves]. The shape and level of the aggregation curves in the presence of AG-modified polymers confirmed that only a small amount of thrombin remained in the PPP samples after incubation. The disaggregation of platelets after 50 s could be explained by the formation of weak platelet-platelet intercellular bonds [41, 42]. In contrast, the platelet aggregation curves in PRP samples incubated with unmodified polymers [Fig. 6(a, b)—black curves] showed very fast platelet aggregation with

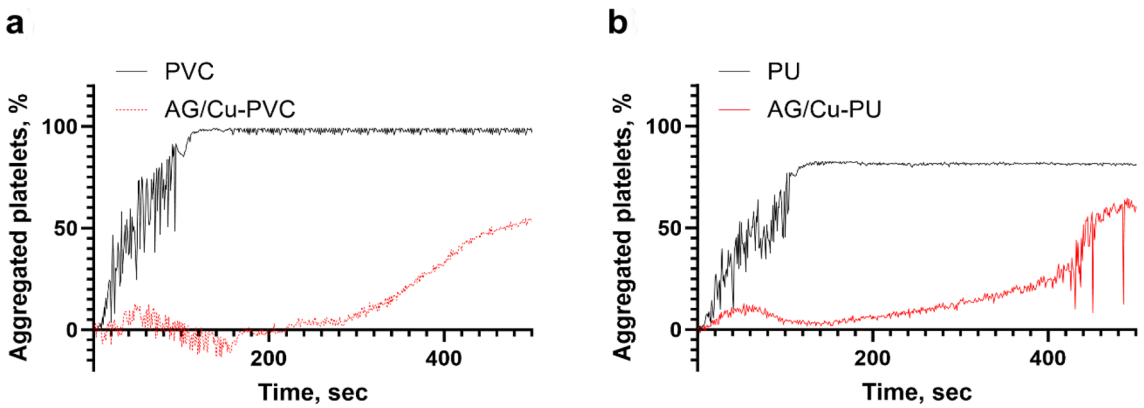

Figure 6: Thrombin-induced platelet aggregation in PRP in the presence of unmodified polymers (black curve) and polymers modified with AG (red); (a) PVC; (b) PU. The kinetic curves are representative of typical experiments, $n = 5$.

simultaneous formation of soluble fibrin. After 100 s the plasma clot which contained the activated platelets and polymerised fibrin was formed.

This results proved that immobilisation of AG onto PVC and PU created the polymer surface that effectively inhibited thrombin activity and prevented thrombin-induced platelet aggregation and could be a valuable approach to preventing blood clotting at the biomaterial-blood interface.

Antimicrobial activity

The antimicrobial activity of AG/Cu-modified polymers was evaluated by testing them against *S. aureus*. Bacterial growth on AG/Cu-modified polymers was analysed in the presence of NO donors (100 μM GSNO/GSH) vs. no NO donors and the data was compared with controls (pristine polymers).

The number of *S. aureus* colonies grown after 2h of exposure to AG/Cu-modified polymers in the presence of NO donors was visibly lower in comparison with the unmodified polymers and AG/Cu-modified materials in the absence of GSNO (Fig. 7).

A one-way ANOVA test was conducted to compare the effectiveness of AG/Cu-modified polymers in comparison with non-modified polymers. The normality checks and Levene's test were carried out and the assumptions were met. The significant difference in the mean values between PVC and AG/Cu-PVC [$F(2,6) = 47.21474$, $p = 2.1324\text{E}{-4}$] and between PU, AG/Cu-PU and AG/Cu-PU + GSNO [$F(2,6) = 73.07123$, $p = 6.13342\text{ E}{-5}$] was found. Post hoc comparisons using the Tukey test revealed a significant difference between PVC and AG/Cu-PVC + GSNO ($p = 2.31\text{ E}{-04}$) and between AG/Cu-PVC and AG/Cu-PVC + GSNO ($p = 7.93\text{ E}{-04}$). These results clearly demonstrated the bactericidal activity of AG/Cu-modified polymers in the presence of 100 μM GSNO/GSH, the NO donor reagents.

A similar pattern in inhibiting bacterial activity was seen with PU modified samples although this effect for AG/Cu-PU is lower (4×10^9 colonies) than for AG/Cu-PVC (3×10^8 colonies) (Fig. 7).

It was noticed that modified polymers showed some antibacterial activity without NO donor although it was much lower than in the presence of NO donors. This effect could be caused by copper ions attached to the polymer surface which were reported to have some antimicrobial activity [43].

Bacterial viability

In this work, Live/Dead staining combined with confocal laser scanning microscopy (CLSM) was used in the analysis of *S. aureus* bacterial viability after incubation of AG/Cu-modified polymers with *S. aureus* during 2 h in the presence of 100 μM GSNO/GSH (Fig. 8). In the Live/Dead staining assay the bacterial membrane integrity is assessed using dyes, SYTO 9 and propidium iodide. SYTO9 permeates membrane of both dead and living cells, while propidium iodide permeates only membranes of damaged cells; as a result, dead bacteria produce a red fluorescence signal and live bacteria give a green signal.

The results of the viability staining of adherent bacteria were in agreement with the results presented in the previous section on the viability of *S. aureus* in the total inoculum. In Fig. 8 it is demonstrated that after incubation with NO donor there are no remaining live bacteria. Both methods, CFU counting and Live/Dead staining assay showed that AG/Cu-modified polymers exhibited antimicrobial properties in the presence of GSNO donor.

In addition to the Gram-positive bacterium *S. aureus*, the antibacterial properties of AG/Cu-PVC were assessed against the Gram-negative bacterium, *Escherichia coli*. This analysis was conducted following the incubation of AG/Cu-modified polymers with *E. coli* for 2 h in the presence of 100 μM GSNO/GSH (Fig. 9). Figure 9(c) shows that AG/Cu-PVC exhibited antibacterial properties against Gram-negative *E. coli*. Although in comparison to *S. aureus*, *E. coli* displayed reduced attachment and tended to float in the liquid phase during confocal microscopy analysis which contributed to a reduction in the focus sharpness of the images obtained.

Discussion

The load of AG immobilised on the surfaces of Cu-modified PVC and Cu-modified PU was 6.05 ± 0.66 μg cm^{-2} and 6.66 ± 0.15 μg cm^{-2}, respectively.

In the spectra of pDA-PVC, the peaks observed in the region between 1500–1600 cm^{-1} are attributed to the overlapping C=C stretching vibrations from the indole ring of pDA and, by different authors, to N–H scissoring vibrations or C=N vibrations thus presenting evidence of pDA formation [44, 45]. The observed shifts and the emergence of new IR bands in the range 1600–1400 cm^{-1} in the Cu/pDA-PVC spectra suggest intricate interactions between copper and the pDA matrix. Specifically, the presence of a peak at 1565 cm^{-1} likely results from copper's coordination with nitrogen-containing groups within pDA. The transition of the peak from 1524 cm^{-1} to 1530 cm^{-1} further underscores structural modifications, possibly through copper's coordination with phenolic or amine functionalities. The disappearance of peaks at 1512 cm^{-1} and 1497 cm^{-1} in the Cu/pDA-PVC spectrum highlights more profound structural changes within pDA, potentially reflecting the modification or loss of specific aromatic or amine groups following copper interaction. Additionally, the shift of a peak from 1468 cm^{-1} to 1486 cm^{-1} suggests modifications in the C–H bending vibrations or changes in the electronic environment of pDA's aromatic system, while the absence of the 1456 cm^{-1} peak confirms the

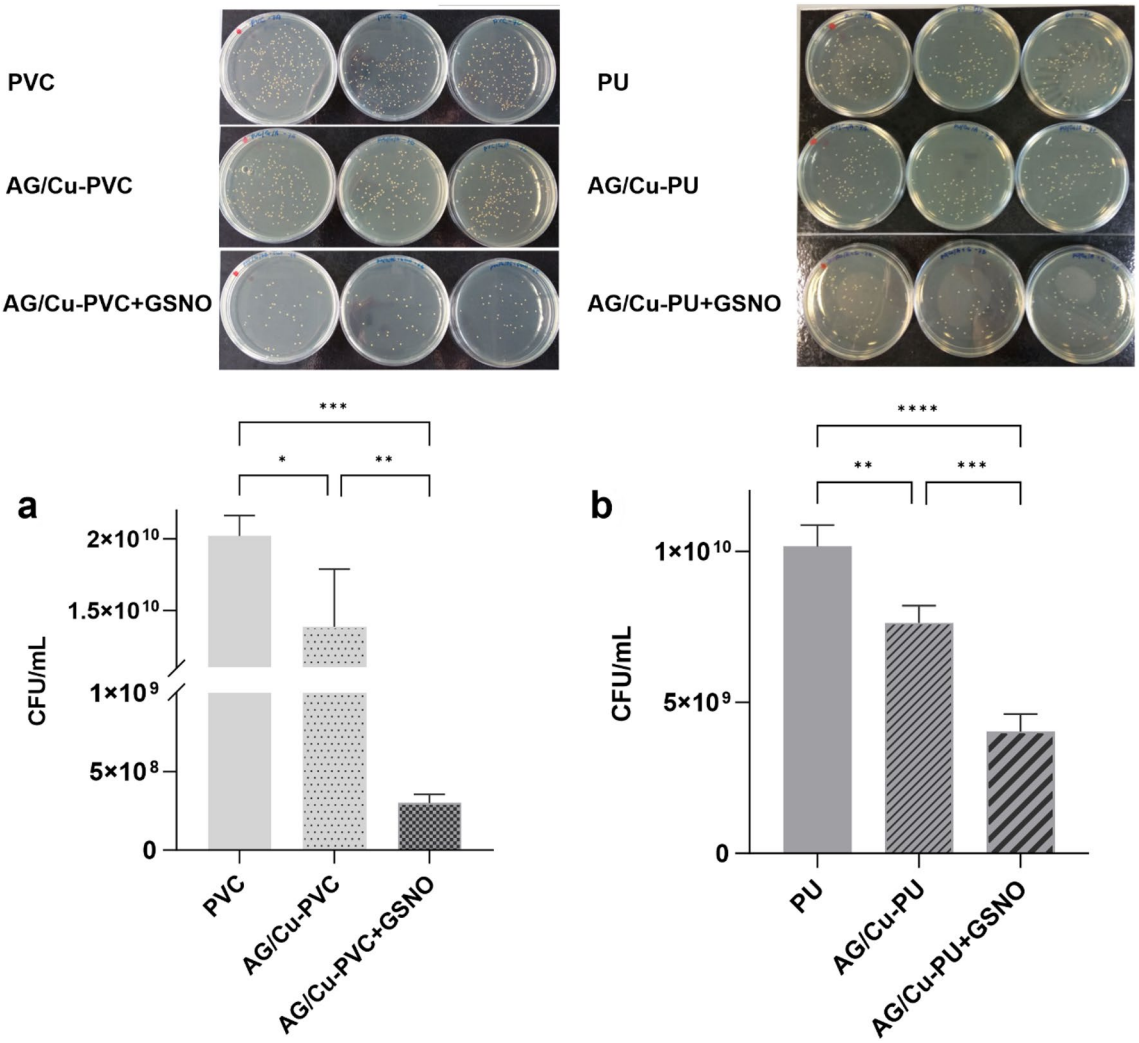

Figure 7: The antimicrobial effect of AG/Cu-PVC (a) and AG/Cu-PU (b) on *S. aureus* after 2-h incubation with 100 μM GSNO/GSH in PBS. In the absence of GSNO/GSH, the AG/Cu-modified polymers did not significantly reduce the number of *S. aureus* colonies in comparison with uncoated polymers. The values are mean of $n = 3$ measurements ± SD. *$p < 0.05$, **$p < 0.01$, ***$p < 0.001$, ****$p < 0.0001$.

structural impact of copper, altering aliphatic C–H groups or methylene chains.

Upon further modification with AG (AG/Cu/pDA-PVC), the appearance of a broad band centred at 3333 cm^{-1} denotes the overlapping stretching vibrations of pDA's phenolic OH groups and the NH aliphatic amine groups from AG, indicating the formation of covalent bonds between AG and polydopamine. This is further supported by the peak at 1605 cm^{-1}, attributed to the formation of –C=N– bonds through Michael addition or Schiff base reactions, which evidences the covalent attachment of AG to the polymer surface. The intensification of the peak region between 1900 and 1300 cm^{-1} post-AG immobilisation underscores the covalent bond formation, marking a significant alteration in the polymer's surface chemistry.

In the spectrum of pristine PU, the characteristic stretching vibration bands of N–H and C–H at 3333 cm^{-1}, 2954 cm^{-1}, 2874 cm^{-1} were observed [Fig. 2(e), spectrum 1]. The bands in the range of 1728–1701 cm^{-1} were attributed to the amide I group characteristic of the urethane structure of PU. An amide II bond associated with in-plane N–H bending vibration of amide group was detected at 1531 cm^{-1}. The spectra of PU modified with Cu and AG [Fig. 2(e), spectra 2 and 3] look similar to the spectrum of the non-modified PU which could be explained by overlapping of the main peaks of the PU matrix with similar functional groups in pDA and AG. Nevertheless, the increased intensity of 3333 cm^{-1} peak and a shoulder peak appearing after the PU surface modification with pDA [Fig. 2(f). spectra 2 and 3], confirm the formation of the covalent bond between AG and pDA on the PU surface, similar to PVC.

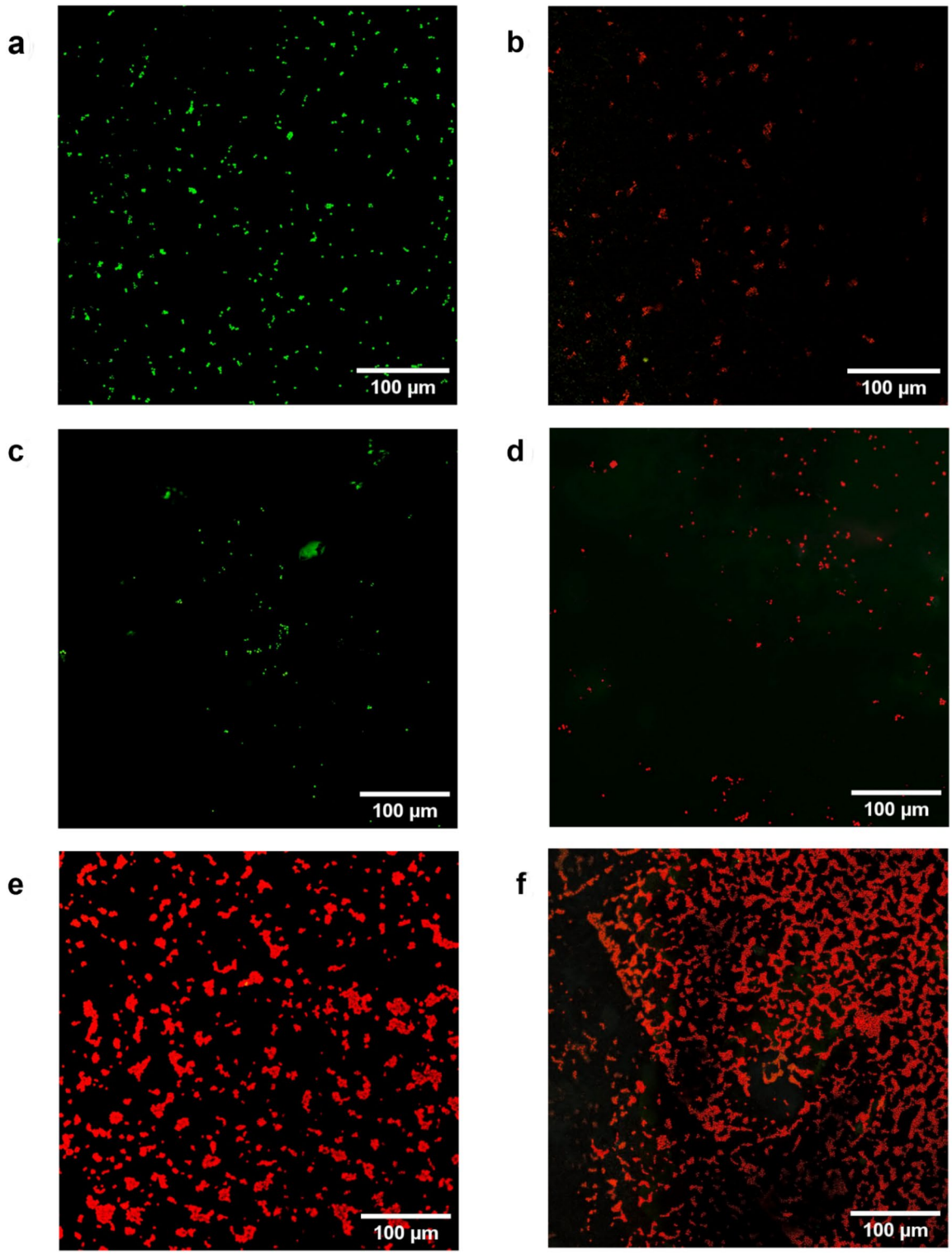

Figure 8: CLSM images of *S. aureus* biofilm on polymer surfaces with Live/Dead staining. The green signal is due to the dye SYTO9, indicating alive cells while the red signal is due to propidium iodide which marks the dead cells. (a) live *S. aureus* on PVC; (b) dead *S. aureus* on PVC; (c) live *S. aureus* on PU; (d) dead *S. aureus* on PU; (e) *S. aureus* biofilm on AG/Cu-PVC after 2-h incubation of the bacterial inoculum with the polymer and 100 µM GSNO/GSH; (f) *S. aureus* biofilm on AG/Cu-PU after 2-h incubation of the bacterial inoculum with the polymer and 100 µM GSNO/GSH. Controls: (a), (c) *S. aureus* alive and (b), (d) *S. aureus* dead.

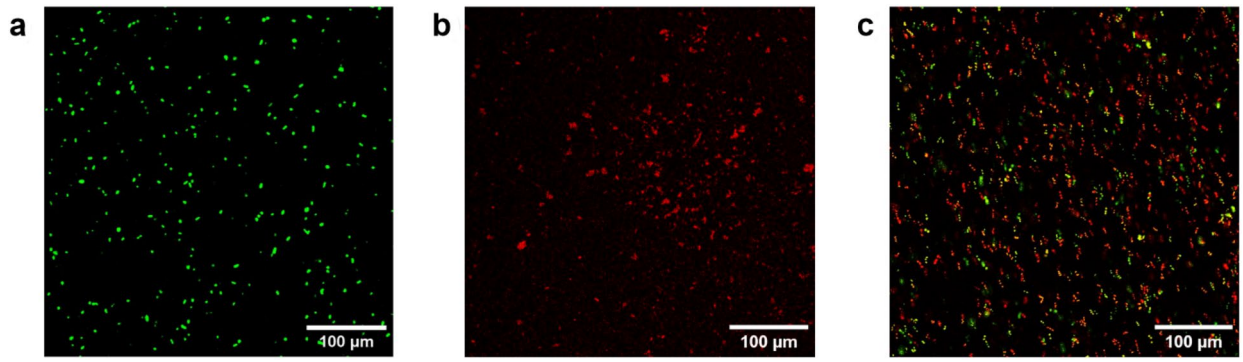

Figure 9: CLSM images of *E. coli* biofilm on PVC surface with Live/Dead staining. The green signal is due to the dye SYTO9 indicating, alive cells while the red signal is due to propidium iodide which marks the dead cells. (a) live *E. coli* on PVC; (b) dead *E. coli* on PVC; (c) *E. coli* biofilm on AG/Cu-PVC after 2-h incubation of the bacterial inoculum with the polymer and 100 µM GSNO/GSH. Controls: a) control *E. coli* alive, (b) control *E. coli* dead.

The NO flux measured for both AG/Cu-modified polymers in PBS and in human blood plasma is within the desirable physiological range of NO produced by healthy endothelium, $0.5 - 4 \times 10^{-10}$ mol cm^{-2} min^{-1} [4] albeit it is lower in the plasma than in PBS.

AG/Cu-PVC and AG/Cu-PU surfaces showed significant reduction of both platelet adhesion and activation, indicating an enhanced haemocompatibility. This effect is characterised by a marked decrease in the number of adhered and spread platelets, as well as the formation of platelet–fibrin aggregates, compared to the unmodified polymer surfaces. The observed platelets on AG-modified surfaces were primarily round-shaped and devoid of pseudopodia, further signifying reduced activation and adhesion.

The thrombin inhibiting activity of the AG/Cu-modified polymers was confirmed in both buffer solutions and human blood plasma, with a notable reduction in thrombin activity after incubation with the modified polymers. This indicates successful functionalisation of the polymers with AG, enhancing their antithrombotic properties.

AG-modified polymers showed a significant reduction in thrombin-induced platelet aggregation, leading to slower fibrin formation compared to the rapid aggregation seen with unmodified polymers. This highlights the effectiveness of AG immobilisation in reducing thrombogenicity.

The antibacterial efficacy of AG/Cu-modified polymers was assessed using experiments with *S. aureus*, revealing that bacterial growth on these modified surfaces was significantly reduced in the presence of GSNO/GSH compared to unmodified and AG/Cu-modified samples without GSNO. A decrease in *S. aureus* colonies was observed on AG/Cu-modified PVC and PU when exposed to GSNO, demonstrating the bactericidal effect of the AG/Cu modifications enhanced by GSNO/GSH. We also observed modest antibacterial activity of modified polymers also without NO donors, which could be explained by the antimicrobial properties of the copper ions integrated into the polymer surfaces, however the presence on NO donors significantly increased antimicrobial activity of polymers.

The bacterial viability study using Live/Dead staining and CLSM confirmed the antimicrobial properties of AG/Cu-modified polymers against gram-positive *S. aureus* by showing predominantly dead bacteria (red fluorescence) in the presence of GSNO.

The antibacterial effect of AG/Cu-PVC against the Gram-negative bacterium, *E. coli* was also assessed.Compared to *S aureus*, *E. coli* demonstrated a lower tendency to adhere to the modified polymer surfaces. A high number of bacteria remained alive in the surrounding medium, while those that did attach to the surface were mostly dead.

The presence of floating *E. coli* decreased the quality of confocal images, making it difficult to focus on the bacteria remaining in the liquid phase. It can be concluded that AG/Cu-modified polymers have the potential to exhibit antibacterial properties against *E. coli*, based on preliminary evidence.

Conclusions

The design of biomedical PVC and PU polymers possessing the dual antithrombotic and antibacterial function was achieved through an innovative surface modification employing copper (II) ions and the direct thrombin inhibitor argatroban.

The effective attachment of copper (II) ions and AG to the polymer surface via the polydopamine immobilisation method was validated using a number of techniques, such as UV/Vis spectrophotometry, FTIR and thrombin inhibition assays, ensuring the integrity of the modification process as well as the target antithrombin biological activity of the modified polymers.

The AG/Cu-modified polymers generated NO in both PBS and human blood plasma, by the catalytic decomposition of

GSNO/GSH as NO donors, at the physiological level associated with endothelial cells, suggesting the potential of these modified polymers to mimic natural antithrombotic mechanisms.

The incorporation of AG into the polymer matrix played a pivotal role in significantly reducing thrombin activity in PBS and more crucially, in human plasma. This effect was paralleled by a marked reduction in platelet adhesion and aggregation on the modified surfaces, addressing key factors in the prevention of thrombus formation.

In addition to their antithrombotic properties, the AG/Cu-modified polymers exhibited pronounced antibacterial activity against *S. aureus*, especially in the presence of GSNO. The modified polymers also exhibited a lesser antibacterial effect on *E. coli*.

The comprehensive evaluation of AG/Cu-modified PVC and PU polymers through NO generation, platelet adhesion, thrombin inhibition, platelet aggregometry and antibacterial properties confirms their enhanced antithrombotic and antibacterial functions.

Taken together, these results prove the dual functionality of the AG/Cu(II) modified polymer surfaces confirming that such modification of polymers emerges as a promising approach to improve the haemocompatibility of materials for blood-contacting medical devices.

Experimental

Materials and methods

Materials

Chemical reagents and materials were purchased from different suppliers as follows: polyvinylchloride film (PVC, thickness 0.2 mm), from Goodfellow Cambridge Ltd, Huntingdon, UK; polyurethane film (PU, thickness 80 μm), from Delstar International Ltd, Brough, UK; phosphate buffered saline tablets (PBS), from MP Biomedicals, Illkirch-Graffenstaden, France; dopamine hydrochloride (DA), tris(hydroxymethyl)aminomethane (Tris), S-nitrosoglutathione (GSNO), L-glutathione reduced (GSH), copper (II) chloride dihydrate ($CuCl_2 \cdot 2H_2O$), argatroban monohydrate (AG), absolute ethanol (99% +), Tween 80, sodium nitrite, sodium nitrate, human blood plasma and bovine serum from Sigma-Aldrich, St. Louis, USA; Triton X-100 from Fisher Scientific, Hampton, NH, USA; and thrombin and thrombin-specific chromogenic substrate S2238 from Sigma, USA. Aggregometer AP2110 was purchased from JSC Solar, Minsk, Belarus. Live/Dead BacLight Bacteria viability kit was purchased from Invitrogen (Thermo Fisher Scientific, USA). DPX mountant was purchased from Surechem Products, Suffolk, UK. All solutions were prepared with 18 MΩ cm^{-1} deionised (DI) water obtained using a Milli-Q system (Millipore Corp., Billerica, MA, USA). No trace of Cu ions was detected in DI water by inductively coupled plasma—mass spectrometry (ICP-MS).

Preparation of Cu-modified PVC and PU polymeric discs with immobilised AG

Copper-modified PVC and PU discs with the diameter $d = 1.3$ cm were prepared as described previously [14]. Briefly, PVC and PU discs were immersed into Tris–HCl buffer solution (10 mM, pH 8.5) containing dopamine (10.5 mM) and copper salt (3 mM $CuCl_2 \cdot 2H_2O$) for 24 h at room temperature (RT) under continuous stirring in the dark. The total volume of the solution was 1 mL per disc. Copper ions were fixed on the polymer surface via polydopamine film formed under these conditions. After sonication and rinsing with DI water the discs were air-dried or further used for AG immobilisation. The immobilisation of AG was performed according to a modified method described by Lu and co-authors [46], however because our polymers were treated with dopamine the Cu-modified discs were placed in a 24-well plate with Tris–HCl buffer (10 mM, pH 8.5) for 15 min and further incubated with a 500 μL solution of 0.1 mg mL^{-1} AG in Tris–HCl buffer overnight. The polymeric discs then were rinsed three times with DI water and sonicated in DI water to remove unbound AG. The discs thus prepared were denoted as AG/Cu-modified PVC and AG/Cu-modified PU.

Evaluation of the quantity of AG grafted onto PVC and PU polymeric disc

The quantity of bound AG was estimated by the difference in the absorbance of AG solution before and after incubation with polymers. The concentration of AG solution was measured spectrophotometrically by UV absorption at 333 nm using the molar extinction coefficient of 5000 M^{-1} cm^{-1} [37].

Fourier transform infrared spectroscopy (FTIR) for the analysis of the surface chemical structure of AG/copper-modified polymers

To confirm pDA, Cu and AG binding to the polymer surface, the chemical structure of the coatings was studied with FTIR using a PerkinElmer Spectrum 65 FT-IR Spectrometer equipped with a UATR accessory in the 650–4000 cm^{-1} range. The method allows the identification of chemical bonds and functional groups present of the surface that could indicate the new bond formation during the modification steps. The discs of pristine and AG/Cu-modified polymers were placed on the sample holder and FTIR spectra were obtained in a transmittance mode averaging eight scans with a resolution of 8 cm^{-1}.

Blood sampling

Fresh human plasma from healthy volunteers was used to perform haemocompatibility studies and for the preparation of platelet-rich plasma (PRP). Venous blood of healthy volunteers ($n = 3$) of both sexes aged from 25 to 35 years who had not taken any medication for 7 days was collected into a 38 g L^{-1} sodium citrate solution (9:1 v/v blood to sodium citrate). PRP was prepared by centrifugation of blood at 200×*g* for 20 min at 23 °C. To obtain platelet-poor plasma (PPP), blood was spun down at 450×*g* for 30 min [47]. The volunteers signed informed consent prior to blood sampling according to the Helsinki declaration. This study was approved by Ethics Committee of the University of Brighton (04.01.2018; in this project the tier-2 approved PaBS Blood Donor Register was used) and Palladin Institute of Biochemistry, Kyiv (05.11.2018, N18). The informed consent and ethical approval are in place. Blood samples for the preparation of PRP were used within 2h of their collection to avoid any activation of platelets or clotting factors. PPP samples were fresh-frozen and stored at − 20 °C no longer than two months. Commercially available human blood plasma (Sigma, USA) was used in the NO generation tests.

Scanning electron microscopy (SEM) of modified polymers after incubation with platelets

After incubation with platelet-rich plasma PRP, the AG/Cu-modified discs were rinsed with PBS, fixed with 500 µL 3% glutaraldehyde (GA) in 0.05 M Tris–HCl buffer, pH 7.4 at RT for 1h. Discs were further dried in a series of ethanol/water solutions by incubation in each ethanol dilution (30%, 50%, 70% and 90% of v/v ethanol in water) for 30–60 min. The drying procedure was completed with absolute ethanol and the discs were left on the lab bench until further use. Prior to SEM analysis, the polymer discs were placed onto stubs and ion-sputtered with palladium. The electron microscopy examination of samples was performed with a Zeiss SIGMA field emission gun scanning electron microscope (FEG-SEM) using a Zeiss in-lens secondary electron detector. The FEG-SEM working conditions were as follows: accelerating voltage of 5 kV and the working distance of 8.5–9.0 mm. At least three samples of each specimen were examined by SEM and the representative images of each are presented in this work.

Nitric oxide release measurements

The NO release catalysed by Cu-modified polymers was examined by ion-selective microelectrodes used for independent measurement of both nitrite and nitrate ions with the Arrowstraight™ Nitric Oxide (NO_2^-/NO_3^-) measurement system (Lazar Research Laboratories, Los Angeles, CA, USA). The GSNO stock solution of 500 µM in PBS was freshly prepared and its concentration was verified spectrophotometrically by measuring the absorption of the SNO group at 335 nm using the molar extinction coefficient of 922 M^{-1} cm^{-1}. The stock solution of L-glutathione reduced (GSH) in PBS (500 µM) was stored in a fridge. NO generation catalysed by AG/Cu-modified polymers was studied in PBS and in human plasma. The polymer discs were placed at the bottom of a 24-well plate and 500 µL of PBS solution was added to each well to equilibrate polymers for 5 min in PBS prior to adding the reagents. Afterwards, the discs were incubated with 1 mL of 100 µM GSNO and 100 µM GSH in PBS or human plasma at 37 °C for 1h with gentle mixing in an orbital shaker. L-Glutathione (GSH) was added as a reducing agent because it is present in blood but not in plasma. During NO measurements, all solutions containing GSNO were shielded from light by foil as light greatly decreases the half-life of GSNO. In the experiments with incubation of the polymer discs in the blood plasma, discs were subsequently removed, and the remaining plasma was spun down using a filtration cartridge with 10 kDa molecular weight cut-off (Amicon Centrifugal Filters, Merck) according to manufacturer's instructions for measuring NO release in biological fluids. After centrifugation, 200 µL of filtrate from each tube was injected into the Arrowstraight™ system to measure NO_2^- and NO_3^- concentrations. The generation of NO from GSNO catalysed by AG/Cu-modified polymers was calculated by summation of the concentrations of NO_2^- and NO_3^- in each sample assuming that the two-side surface area of each disc with $d = 1.3$ cm was 2.65 cm^2. As a standard, serial dilutions of 0.1 M sodium nitrite and 0.1 M sodium nitrate solutions were used. NO measurements were performed according to the manufacturer's instructions using the software provided. All measurements were performed in triplicate.

Thrombin activity inhibition by AG-modified polymers in Tris buffer

AG/Cu-modified polymer discs were incubated with 200 µL of human thrombin (final activity 0.32 NIH mL^{-1}) in 0.05 M Tris–HCl buffer, 0.13 M NaCl, pH 7.4 for 20 min. The remaining thrombin activity was measured using the thrombin-specific chromogenic substrate S2238 (H–D-Phe-Pip-Arg-pNA). The total volume of the solution was 250 µL. The coloured product, p-nitroaniline (pNA) generated during the substrate cleavage by thrombin (thrombin activity) was measured at 405 nm using Reader Multiscan (Thermo Fisher, USA) during 10 min. The residual thrombin activity was calculated as a percentage of the control (0.32 NIH mL^{-1} of thrombin in Tris buffer).

Thrombin activity inhibition by AG-modified polymers in blood plasma

Each disc of pristine polymer and AG/Cu-modified polymer was placed in 200 µL of human blood plasma, diluted 1:20 with Tris buffer (as in 2.9). A specific enzyme from *Echis multisquamatis*

snake venom was added to activate the plasma prothrombin into thrombin [48] and the samples were incubated for 20 min. After incubation, the thrombin activity in the samples was measured using the thrombin-specific chromogenic substrate S2238 as described in 2.9. The thrombin activity in the plasma samples was measured and compared with the control. Plasma incubated with specific enzyme from *Echis carinatus multisquamatis* (multiscale saw-scaled viper) snake venom for 20 min but without polymer discs was used as the control.

Platelet aggregometry

Platelet aggregation was evaluated by measuring the turbidity of human PRP [49]. Discs of AG-modified polymers were placed at the bottom of the aggregometer sample tubes and 250 µL of PRP was added to each tube. Then 25 µL of 0.025 M $CaCl_2$ solution was added to each tube and platelets were activated by adding 25 µL of 5 NIH mL^{-1} of thrombin. The turbidity measurements were carried out with gentle continuous mixing by the magnetic stirrer during the measurement time. The platelet aggregation rate and % of aggregation, in samples with modified and non-modified discs measured at the same conditions, were compared.

Antibacterial studies

The minimum bactericidal concentration (MBC) *S. aureus* in 10 mL tryptone soya broth was incubated overnight at 37 °C with shaking, then washed twice and the pellet re-suspended in 2 mL of PBS. The culture was split into four 500 µL aliquots containing either PBS with 0.005% Tween 80 or 50 µL of 1 mM GSH and 50 µL of 1 mM GSNO and 400 µL of sterile PBS with 0.005% Tween 80. 50 µL of bacterial suspension was applied to modified PVC and PU discs (in triplicate). Controls were uncoated PVC and PU discs. These were allowed to stand at 37 °C for 2 h. After 2-h incubation, the discs were moved to Bijou bottles containing sterile glass beads and 1 mL PBS. The bottles were vortexed for 30 s to remove adherent bacteria, ten-fold serially diluted and 100 µL aliquots spread onto tryptone soya agar. These were inverted and incubated overnight at 37 °C and the resultant colonies counted and converted to colony forming units (CFU) per mL.

Bacterial viability assessment by Live/Dead BacLight bacterial viability assay (Live/Dead staining) combined with Laser scanning confocal microscopy (CLSM)

Staphylococcus aureus or *Escherichia coli* in 10 mL tryptone soya broth was incubated overnight at 37 °C with shaking, then washed twice and the pellet re-suspended in 2 mL 0.85% NaCl solution. AG/Cu-modified polymer discs were placed into wells of a 24-well plate individually. The bacterial suspension (50 µL) was then inoculated onto the disc surfaces and incubated at 37 °C for 2 h. After the incubation, the excess of fluid was removed from discs with a pipette. Discs were placed onto microscope slides. The staining reagent containing SYTO 9 and propidium iodide (PI) fluorophores was prepared according to the manufacturer's instructions and dropped (25 µL) on the surface of the discs. Glass cover slips (22 mm × 22 mm) and DPX mountant were used to seal the samples.

The control PVC and PU discs with live *S. aureus* or *E. coli* and the control PVC and PU discs with *S. aureus* or *E. coli* treated with 70% propanol-2 to kill the *S. aureus* or *E. coli* were also stained with the Live/Dead staining kit. The viability of the biofilm samples was assessed by imaging the samples with a Leica TCS SP5 Confocal Laser Scanning Microscope (Leica Microsystems, Mannheim, Germany). Excitation was performed using Argon laser (488 nm) for both dyes with power set to 25%. SYTO 9 emission was measured at 510 to 550 nm and PI emission at 610 to 650 nm. Z-stack images were acquired at 1-µm intervals (20–30 µm thick) and orthogonal projections were constructed. Three samples of each specimen were examined and the representative images of each are presented in this work.

Statistical analysis

GraphPad Prism 9.5 (GraphPad Software, San Diego, California, USA) was utilised for statistical analysis. Statistical significance was defined as p-values ≤ 0.05. To determine statistical significance, we employed one-way ANOVA followed by Tukey's post hoc multiple-comparison test. In the figures, data are presented as means ± standard deviation. All experiments were conducted at least in triplicate.

Acknowledgments

The authors acknowledge the DelStar Company for donating PU films.

Author contributions

Liana Azizova: conceptualization, methodology, formal analysis, investigation, writing—original draft, writing—review & editing, visualization, project administration, funding acquisition. Volodymyr Chernyshenko: methodology, formal analysis, investigation. Daria Korolova: methodology, formal analysis, investigation. Iain U. Allan: Conceptualization, writing—review & editing. Sergey Mikhalovsky: conceptualization, writing—review & editing, supervision. Lyuba Mikhalovska: conceptualization, formal analysis, writing—original draft, writing—review & editing, supervision, project administration.

Funding

This work was supported by the Marie Skłodowska-Curie Action of the European Union (H2020-MSCA-IF-2016, Grant Agreement No. 749207).

Data availability

The datasets used and analysed during the current study are available from the corresponding author upon reasonable request.

Declarations

Conflict of interest The authors declare that they have no known competing financial interests or personal relationships that could have appeared to influence the work reported in this paper.

Ethical approval

This study utilised human blood obtained from donors as well as commercially available human plasma. The volunteers signed informed consent prior to blood sampling according to the Helsinki declaration. This study was approved by Ethics Committee of the University of Brighton (04.01.2018; in this project the tier-2 approved PaBS Blood Donor Register was used) and Palladin Institute of Biochemistry, Kyiv (05.11.2018, N18). The informed consent and ethical approval are in place.

Open Access

References

1. C. Sperling, K. Salchert, U. Streller, C. Werner, Covalently immobilized thrombomodulin inhibits coagulation and complement activation of artificial surfaces in vitro. Biomaterials **25**(21), 5101 (2004)
2. M.C. Wyers, M.D. Phaneuf, E.M. Rzucidlo, M.A. Contreras, F.W. LoGerfo, W.C. Quist, In vivo assessment of a novel Dacron surface with covalently bound recombinant Hirudin. Cardiovasc Pathol **8**(3), 153 (1999)
3. J. Yu, E. Brisbois, H. Handa, G. Annich, M. Meyerhoff, R. Bartlett, T. Major, The immobilization of a direct thrombin inhibitor to a polyurethane as a nonthrombogenic surface coating for extracorporeal circulation. J. Mater. Chem. B **4**(13), 2264 (2016)
4. A. de Mel, F. Murad, A.M. Seifalian, Nitric oxide: A guardian for vascular grafts? Chem. Rev. **111**(9), 5742 (2011)
5. M.A. Elnaggar, D.K. Han, Y.K. Joung, Nitric oxide releasing lipid bilayer tethered on titanium and its effects on vascular cells. J. Ind. Eng. Chem. **80**, 811 (2019)
6. M.A. Elnaggar, S.H. Seo, S. Gobaa, K.S. Lim, I.-H. Bae, M.H. Jeong, D.K. Han, Y.K. Joung, Nitric oxide releasing coronary stent: A new approach using layer-by-layer coating and liposomal encapsulation. Small **12**(43), 6012 (2016)
7. F. Kabirian, P. Brouki Milan, A. Zamanian, R. Heying, M. Mozafari, Nitric oxide-releasing vascular grafts: A therapeutic strategy to promote angiogenic activity and endothelium regeneration. Acta Biomater. **92**, 82 (2019)
8. S. Paul, S. Pan, A. Mukherjee, P. De, Nitric oxide releasing delivery platforms: Design, detection, biomedical applications, and future possibilities. Mol. Pharm. **18**(9), 3181 (2021)
9. J. Rao, H. Pan Bei, Y. Yang, Y. Liu, H. Lin, X. Zhao, Nitric oxide-producing cardiovascular stent coatings for prevention of thrombosis and restenosis. Front Bioeng. Biotechnol. **8**, 578 (2020)
10. J. Pant, M.J. Goudie, S.P. Hopkins, E.J. Brisbois, H. Handa, Tunable nitric oxide release from S-nitroso-N-acetylpenicillamine via catalytic copper nanoparticles for biomedical applications. ACS Appl. Mater. Interfaces **9**(18), 15254 (2017)
11. Q. Tu, X. Shen, Y. Liu, Q. Zhang, X. Zhao, M.F. Maitz, T. Liu, H. Qiu, J. Wang, N. Huang, Z. Yang, A facile metal–phenolic–amine strategy for dual-functionalization of blood-contacting devices with antibacterial and anticoagulant properties. Mater. Chem. Front. **3**(2), 265 (2019)
12. Z. Yang, Y. Yang, L. Zhang, K. Xiong, X. Li, F. Zhang, J. Wang, X. Zhao, N. Huang, Mussel-inspired catalytic selenocystamine-dopamine coatings for long-term generation of therapeutic gas on cardiovascular stents. Biomaterials **178**, 1 (2018)
13. M. Elnaggar, M.L. Hasan, S.H. Bhang, Y.K. Joung, Endothelial cell-derived tethered lipid bilayers generating nitric oxide for endovascular implantation. ACS Appl. Bio Mater. **4**(8), 6381 (2021)
14. L. Azizova, S. Ray, S. Mikhalovsky, L. Mikhalovska, Development of Cu-modified PVC and PU for catalytic generation of nitric oxide. Colloids Interfaces **3**(1), 33 (2019)
15. R. Biran, D. Pond, Heparin coatings for improving blood compatibility of medical devices. Adv. Drug Deliv. Rev. **112**, 12 (2017)
16. S.M. Bates, J.I. Weitz, New anticoagulants: beyond heparin, low-molecular-weight heparin and warfarin. Br. J. Pharmacol. **144**(8), 1017 (2005)
17. C.J. Lee, J.E. Ansell, Direct thrombin inhibitors *Br.* J. Clin. Pharmacol. **72**(4), 581 (2011)
18. M. Beiderlinden, T. Treschan, K. Görlinger, J. Peters, Argatroban in extracorporeal membrane oxygenation. Artif. Organs **31**(6), 461 (2007)

19. S.-S. Fu, J.-P. Ning, X.-H. Liao, X. Fu, Z.-B. Yang, Preparation and characterization of a thrombin inhibitor grafted polyethersulfone blending membrane with improved antithrombotic property. RSC Adv. **5**(116), 95710 (2015)
20. X. Fu, J.-P. Ning, Synthesis and biocompatibility of an argatroban-modified polysulfone membrane that directly inhibits thrombosis. J. Mater. Sci. Mater. Med. **29**(5), 66 (2018)
21. T.C. Major, E.J. Brisbois, A.M. Jones, M.E. Zanetti, G.M. Annich, R.H. Bartlett, H. Handa, The effect of a polyurethane coating incorporating both a thrombin inhibitor and nitric oxide on hemocompatibility in extracorporeal circulation. Biomaterials **35**(26), 7271 (2014)
22. M. Menk, P. Briem, B. Weiss, M. Gassner, D. Schwaiberger, A. Goldmann, C. Pille, S. Weber-Carstens, Efficacy and safety of argatroban in patients with acute respiratory distress syndrome and extracorporeal lung support. Ann Intens. Care **7**(1), 82 (2017)
23. S. Nishi, Y. Nakayama, H. Ishibashi-Ueda, Y. Masato, Occlusion of canine aneurysms using microporous self-expanding stent grafts: Long-term follow-up. Clin. Neurol. Neurosurg.. **122**, 34 (2014)
24. Y. Zhang, J. Ning, P. Veeraragoo, Y. Li, S. Dai, Hemodialysis with a dialyzer loaded with argatroban may be performed in vivo without a systemic anticoagulant. Blood Purif. **33**(4), 300 (2012)
25. Y. Dai, S. Dai, X. Xie, J. Ning, Immobilizing argatroban and mPEG-NH_2 on a polyethersulfone membrane surface to prepare an effective nonthrombogenic biointerface. J. Biomater. Sci. Polym. Ed. **30**(8), 608 (2019)
26. C. Miao, L. Wang, Y. Shang, M. Du, J. Yang, J. Yuan, Tannic acid-assisted immobilization of copper(II), carboxybetaine, and argatroban on poly(ethylene terephthalate) mats for synergistic improvement of blood compatibility and endothelialization. Langmuir **38**(50), 15683 (2022)
27. T. He, J. He, Z. Wang, Z. Cui, Modification strategies to improve the membrane hemocompatibility in extracorporeal membrane oxygenator (ECMO). Adv. Compos. Hybrid Mater. **4**(4), 847 (2021)
28. R. Namivandi-Zangeneh, Z. Sadrearhami, A. Bagheri, M. Sauvage-Nguyen, K.K.K. Ho, N. Kumar, E.H.H. Wong, C. Boyer, Nitric oxide-loaded antimicrobial polymer for the synergistic eradication of bacterial biofilm. ACS Macro Lett. **7**(5), 592 (2018)
29. F. Rong, Y. Tang, T. Wang, T. Feng, J. Song, P. Li, W. Huang, Nitric oxide-releasing polymeric materials for antimicrobial applications: a review. Antioxidants **8**(11), 556 (2019)
30. C. Warden, J. Tan, K.M. Piell, N. Janakiraman, M.E. Meyerhoff, J.M. Steinbach-Rankins, M.P. Cole, S. Gudhimella, A novel, nitric oxide-releasing elastomeric chain for antimicrobial action: proof of concept. Mater. Res. Express **8**(9), 095309 (2021)
31. J. Park, J. Kim, K. Singha, D.-K. Han, H. Park, W.J. Kim, Nitric oxide integrated polyethylenimine-based tri-block copolymer for efficient antibacterial activity. Biomaterials **34**(34), 8766 (2013)
32. M.J. Duncan, P.S. Wheatley, E.M. Coghill, S.M. Vornholt, S.J. Warrender, I.L. Megson, R.E. Morris, Antibacterial efficacy from NO-releasing MOF–polymer films. Mater. Adv. **1**(7), 2509 (2020)
33. J. Lee, S.P. Hlaing, J. Cao, N. Hasan, H.-J. Ahn, K.-W. Song, J.-W. Yoo, In Situ hydrogel-forming/nitric oxide-releasing wound dressing for enhanced antibacterial activity and healing in mice with infected wounds. Pharmaceutics **11**, 496 (2019)
34. Z. Sadrearhami, F.N. Shafiee, K.K.K. Ho, N. Kumar, M. Krasowska, A. Blencowe, E.H.H. Wong, C. Boyer, Antibiofilm nitric oxide-releasing polydopamine coatings. ACS Appl. Mater. Interfaces **11**(7), 7320 (2019)
35. D.O. Schairer, J.S. Chouake, J.D. Nosanchuk, A.J. Friedman, The potential of nitric oxide releasing therapies as antimicrobial agents. Virulence **3**(3), 271 (2012)
36. L. Yang, E.S. Feura, M.J.R. Ahonen, M.H. Schoenfisch, Nitric oxide-releasing macromolecular scaffolds for antibacterial applications. Adv. Healthc. Mater. **7**(13), 1800155 (2018)
37. N. Pozzi, Z. Chen, F. Zapata, W. Niu, S. Barranco-Medina, L.A. Pelc, E. Di Cera, Autoactivation of thrombin precursors. J. Biol. Chem. **288**(16), 11601 (2013)
38. G. Socrates, *Infrared and Raman Characteristic Group Frequencies: Tables and Charts* (Wiley, Hoboken, 2004)
39. R.J. Petrovan, J.W.P. Govers-Riemslag, G. Nowak, H.C. Hemker, J. Rosing, G. Tans, Purification and characterization of multisquamase, the prothrombin activator present in echis multisquamatus venom. Thromb. Res. **88**(3), 309 (1997)
40. D.A. Solovjov, T.N. Platonova, U. Tp, Purification and characterization of ecamulin: A new prothrombin activator from the echis multisquamatus snake venom. Biochemistry **61**, 785 (1996)
41. D.M. Monroe, M. Hoffman, H.R. Roberts, Platelets and thrombin generation. Arterioscler. Thromb. Vasc. Biol. **22**(9), 1381 (2002)
42. P.P. Wadowski, B. Eichelberger, C.W. Kopp, J. Pultar, D. Seidinger, R. Koppensteiner, I.M. Lang, S. Panzer, T. Gremmel, Disaggregation following agonist-induced platelet activation in patients on dual antiplatelet therapy. J. Cardiovasc. Transl. Res. **10**(4), 359 (2017)
43. M. Vincent, R.E. Duval, P. Hartemann, M. Engels-Deutsch, Contact killing and antimicrobial properties of copper. J. Appl. Microbiol. **124**(5), 1032 (2018)
44. D.R. Dreyer, D.J. Miller, B.D. Freeman, D.R. Paul, C.W. Bielawski, Elucidating the structure of poly(dopamine). Langmuir **28**(15), 6428 (2012)
45. R.A. Zangmeister, T.A. Morris, M.J. Tarlov, Characterization of polydopamine thin films deposited at short times by autoxidation of dopamine. Langmuir **29**(27), 8619 (2013)
46. L. Lu, Q.-L. Li, M.F. Maitz, J.-L. Chen, N. Huang, Immobilization of the direct thrombin inhibitor-bivalirudin on 316L stainless steel via polydopamine and the resulting effects on hemocompatibility in vitro. J. Biomed. Mater. Res. A **100A**(9), 2421 (2012)

47. V. Chernyshenko, K. Shteinberg, N. Lugovska, M. Ryzhykova, Preparation of highly-concentrated autologous platelet-rich plasma for biomedical use. Ukr. Biochem. J. **91**(2), 19 (2019)
48. D.S. Korolova, T.M. Chernyshenko, O.V. Gornytska, V.O. Chernyshenko, T.N. Platonova, Meizothrombin preparation and its role in fibrin formation and platelet aggregation. Adv. Biosci. Biotechnol. **5**(7), 588 (2014)
49. M. Cattaneo, C. Cerletti, P. Harrison, C.P.M. Hayward, D. Kenny, D. Nugent, P. Nurden, A.K. Rao, A.H. Schmaier, S.P. Watson, F. Lussana, M.T. Pugliano, A.D. Michelson, Recommendations for the standardization of light transmission aggregometry: A consensus of the working party from the platelet physiology subcommittee of SSC/ISTH. J. Thromb. Haemost. **11**(6), 1183 (2013)